

Received 11 September 2025, accepted 16 October 2025, date of publication 22 October 2025, date of current version 29 October 2025.

Digital Object Identifier 10.1109/ACCESS.2025.3624280



Monitoring Hydrogen and Methane Gases in Transformer Oil Using Palladium and Polydimethylsiloxane Coated Fiber Bragg Grating Sensors

FOLAD FAWAD[®]1, (Graduate Student Member, IEEE), SUPAKIT CHOTIGO[®]1, APICHAI BHATRANAND[®]2, SARAYUT YONGPRAPAT³, SANGUAN ANANTATHANASARN⁴, AND RATTANAPORN SUKSOMBOON⁴

¹Department of Electrical Engineering, Faculty of Engineering, King Mongkut's University of Technology Thonburi, Bangkok 10140, Thailand ²Department of Electronic and Telecommunication Engineering, Faculty of Engineering, King Mongkut's University of Technology Thonburi, Bangkok 10140, Thailand

³Fuel Cells and Hydrogen Research and Engineering Center, Pilot Plant Development and Training Institute (PDTI).

King Mongkut's University of Technology Thonburi, Bangkok 10140, Thailand

⁴Furukawa FITEL (Thailand) Company Ltd., Phranakorn Sri Ayutthaya 13210, Thailand

Corresponding author: Apichai Bhatranand (apichai.bha@kmutt.ac.th)

The work of Folad Fawad was supported by the Petchra Pra Jom Klao Doctor Degree Research Scholarship from the King Mongkut's University of Technology Thonburi under Grant No. 13/2565.

ABSTRACT This study presents Fiber Bragg Grating (FBG) sensors coated with palladium (Pd) and polydimethylsiloxane (PDMS) for detecting dissolved hydrogen (H₂) and methane (CH₄) in transformer oil, key indicators of incipient transformer faults. Laboratory evaluations covered concentrations of 5–2146 ppm for H₂ and 3–1551 ppm for CH₄ at 10–90 °C. Gas-induced Bragg wavelength shifts were validated against Dissolved Gas Analysis (DGA) using the Transport X system. The Pd-coated H₂ sensors achieved sensitivities of 0.000487 nm/ppm with 97.04% accuracy and 0.000451 nm/ppm with 99.953% accuracy, while PDMS-coated CH₄ sensors reached 0.00591 nm/ppm with 95.85% accuracy and 0.00226 nm/ppm with 95.03% accuracy. All sensors exhibited strong linearity (R² > 0.91) and excellent repeatability (RSD < 1% above 40 °C). Temperature compensation models were developed to ensure accuracy under varying operational conditions. Compared with previously reported optical gas sensors, the proposed Pd-and PDMS-coated FBG sensors demonstrate superior sensitivity, broad detection range, thermal stability, and cost-effectiveness. These features make them highly promising for real-time, in-situ monitoring of dissolved gases, enabling advanced fault diagnosis and condition-based maintenance in power transformers.

INDEX TERMS Fiber Bragg grating sensors, transformer oil, hydrogen and methane detection, dissolved gas analysis, palladium (Pd), polydimethylsiloxane polymer (PDMS).

I. INTRODUCTION

Oil transformers are essential components in power systems, serving as critical links in power transmission networks. Their reliability depends significantly on the condition of the insulating oil, which can degrade due to faults such as partial discharges or localized overheating. These faults cause thermal and electrical stress on the insulation (oil

The associate editor coordinating the review of this manuscript and approving it for publication was Salvatore Surdo.

and paper), leading to the formation of dissolved gases, including H₂, CH₄, C₂H₂, C₂H₄, C₂H₆, CO, and CO₂ [1], [2], [3]. Dissolved Gas Analysis (DGA) is widely used to assess transformer condition, with hydrogen (H₂) recognized as a key fault indicator due to its early presence in most failure modes [4], [5]. Although hydrogen is typically dissolved in oil, it can also accumulate in the transformer headspace depending on the designs. Real- time monitoring of H₂ is crucial for early fault detection and for preventing severe damage. Several online detection techniques have been



explored, including gas chromatography, electrochemical sensors, photoacoustic spectroscopy, Raman spectroscopy, infrared spectroscopy, and fiber Bragg grating (FBG) sensors [6]. Gas chromatography lacks real-time capability and has a relatively high error margin [7]. Electrochemical sensors suffer from limited lifespan and stability issues in oil-immersed environments [8], [9], [10]. Optical techniques such as photoacoustic, Raman, and infrared spectroscopy are sensitive to environmental factors and often exhibit low selectivity and stability [11], [12], [13]. FBG sensors have emerged as promising alternatives due to their fast response, immunity to electromagnetic interference, and potential for in-situ measurement of dissolved gases such as hydrogen and methane [14]. Jiang et al. [15] enhanced the sensitivity of FBGs through side-polishing, albeit at the cost of mechanical strength. Trouillet et al. [16] and Wang et al. [17] developed long-period fiber grating (LPFG) sensors with significantly higher sensitivity. Basumallick et al. [18] further improved performance using Pd-coated LPFGs, although the long-term stability remained a concern. Recent work has focused on Pd-based and Pd-Cr alloy-coated FBG sensors for in-oil hydrogen monitoring [19], [20], [21]. Recently, researchers have created and modified palladium-chromium ratios of 100:0 (Pd100) and 58:42 (Pd58Cr42) FBG sensor to measure H₂ and CH₄ concentration in transformer oil [21]. In this research, FBG sensors have been developed to monitor transformer oil, and these sensors can measure two key parameters: hydrogen (H₂) and methane (CH₄) concentration in transformer oil. The sensor's notable feature is its ability to perform online measurements for the two parameters mentioned. The sensors design emphasizes simplicity and cost-effectiveness, using readily available materials. The sensor's theoretical background, fabrication process, and experimental procedures are explained in Sections II and III, respectively, while Sections IV cover the experimental results. Finally, the sensor characteristic conclusions are presented in Section V.

II. MEASUREMENT PRINCIPLE

The working principle of an FBG-based hydrogen and methane gas sensors relies on the change in strain or temperature induced by chemical interactions between the gases and the sensor's sensitive coating materials. These interactions cause shifts in the Bragg wavelength (λ_B), governed by [21], [22], [23], [24], and [25]:

$$\lambda_B = 2 \, n_{eff} \, \Lambda \tag{1}$$

where n_{eff} is the effective refractive index of the guided mode in the fiber, and Λ is the grating period. When the FBG sensors are exposed to H_2 or CH_4 , coatings such as palladium (Pd) and polydimethylsiloxane (PDMS) undergo expansion or contraction, applying strain on the FBG, leading to a measurable shift in λ_B . This strain-induced wavelength shift is described as the fractional wavelength shift $(\Delta \lambda_B/\lambda_B)$ due to H_2 and CH_4 strain on the FBG, which can be given

by [21], [22], [23], [24], and [25]:

$$\frac{\Delta \lambda_B}{\lambda_B} = (1 - P)\,\varepsilon = K_\varepsilon \varepsilon \tag{2}$$

where ε is strain caused by gas absorption, K_{ε} is the strain sensitivity coefficient (≈ 0.78 for silica at a wavelength of 1550 nm), P is the effective strain-optic constant (≈ 0.22 for silica at $\lambda = 1550$ nm). In thermally sensitive environments, the Bragg wavelength also shifts due to changes in both the fiber's physical length and refractive index. Thus, the fractional wavelength shift ($\Delta \lambda_B/\lambda_B$) due to the temperature change can be expressed as follows [21], [24], [25], [26]:

$$\frac{\Delta \lambda_B}{\lambda_B} = (\alpha + \zeta) \, dT = K_T \tag{3}$$

where α is the thermal expansion coefficient of the fiber $(\approx 6.5 \times 10^{-6})^{\circ}$ C for silica), ζ is the thermo-optic coefficient $(\approx 0.17 \times 10^{-6})^{\circ}$ C), and K_T is the thermal sensitivity coefficient $(\approx 10 \text{ pm})^{\circ}$ C for silica at 1550 nm).

According to [21], when the sensor is deployed in mineral oil containing hydrogen or methane, the gas-induced expansion or absorption causes a measurable shift in the Bragg wavelength, where $\alpha\delta$ is thermal expansion coefficient temperature influence on the FBG sensor, $\alpha\delta = 7 \times 10^{-6}$ /°C, and $\alpha + \zeta = 6.67 \times 10^{-6}$ /°C. The factor is compensated for in the calculation of the strain. The strain (ε) can be calculated as a function of temperature change (ΔT) in Celsius as [21] and [25].

$$\varepsilon = \frac{\frac{\Delta \lambda_B}{\lambda_B} - \alpha \delta \Delta T}{K_{\varepsilon}} \tag{4}$$

Thus, theoretical Bragg wavelength shift $\Delta \lambda_B$ is given by

$$\Delta \lambda_B = \lambda_B (K_\varepsilon \varepsilon + \alpha \delta \Delta T) \tag{5}$$

In this study, the experimental Bragg wavelength shift $\Delta \lambda_B$ is obtained from the difference of the Bragg wavelength when the sensor is submerged in oil and without oil (in air), as given by:

$$\Delta \lambda_B = \lambda_{B,in\ oil} - \lambda_{B,in\ oir} \tag{6}$$

where $\lambda_{B,in\ oil}$ and $\lambda_{B,in\ air}$ is the Bragg wavelength when the sensor is in oil and in the air (without oil), respectively.

The resonance is often expressed in relative terms as a chemical shift value, defined with respect to the resonance frequency of a standard reference compound. The chemical shift for a specific spin-1/2 nucleus is expressed in parts per million (ppm) using the sample and reference resonance frequencies (in Hz) [27]. Analogously, the fractional wavelength shifts caused by H₂ and CH₄-induced strains on the FBG sensor are also expressed in parts per million (ppm). The numerical value of the wavelength shift (φ) is defined as the ratio of the Bragg wavelength shift ($\Delta \lambda_B$) to the original Bragg wavelength (λ_B), as shown in (7) [27].

$$\varphi = \frac{\Delta \lambda_B}{\lambda_B} \times 10^6 (\text{ppm}) \tag{7}$$



Changes in the calculated strain values resulting from H₂ and CH₄ absorption in oil are used to evaluate and classify the performance of each Bragg grating (FBG) sensor. This study utilizes the advantages of FBGs, known for their high sensitivity to strain, alongside palladium's effective hydrogen absorption and PDMS's ability to absorb methane, to create miniaturized, in-situ sensors for precise gas detection. As illustrated in Fig. 1 and supported by theoretical analysis, when dissolved hydrogen and methane are absorbed by their respective sensitive films (palladium for H₂ and PDMS for CH₄), the resulting external strain alters the FBG structure. This strain alters the optical properties of the fiber, causing a shift in its resonance wavelength.

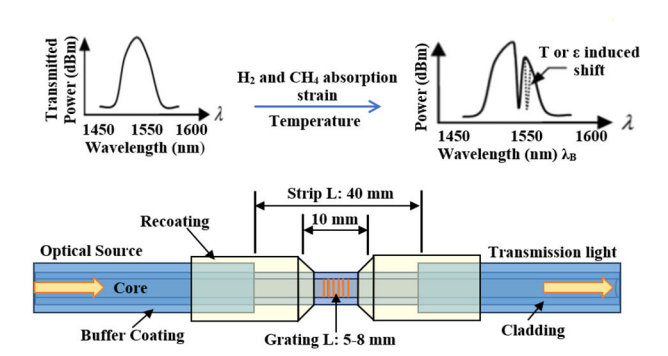


FIGURE 1. Principle of FBG-based hydrogen and methane sensors.

III. EXPERIMENTAL SETUP

A. FABRICATION OF FIBER BRAGG GRATING SENSORS

The design of the single-period Fiber Bragg Grating (FBG) sensors is illustrated in Fig. 2(a). Key specifications a grating length of 10 mm, a grating period of 520 nm for a hydrogen and 550 nm for a methane sensor, and a refractive index of the fibers core of 1.448. The striped length is 40 mm, with a grating region ranging from 5 to 8 mm. The fiber core diameter is $10~\mu\text{m}$, and the cladding diameter is $125~\mu\text{m}$ and coating jacket is $250~\mu\text{m}$ as shown in Fig. 2(a)–(d). However, the drawing is not in scale. The FBG sensor design parameters are summarized in Table 1.

B. COATING FIBER BRAGG GRATING SENSORS

The uncoated region of the FBG sensors was coated with prepared materials: 99.95% pure palladium (Pd) and 99.9% pure PDMS polymer. Palladium, a thermally curable material, is used for hydrogen gas detection, while PDMS is applied for methane gas sensing [28], [29]. Both materials can be easily deposited onto the sensors using dip- and spin-coating methods. The palladium coating was prepared by mixing Pd powder with a cross-linker (curing agent or hardener) in a 10:1 volume ratio. A similar process was used for preparing the PDMS coating. The dip-coating method was selected for its protective properties and its suitability for precise application on microscale optical fiber structures [28]. The step-by-step coating process is illustrated in Fig. 3. Palladium powders and cross-linker were thoroughly mixed for

TABLE 1. Fiber Bragg Grating (FBG) sensor parameters.

Parameters	Values
Wavelength	$\lambda_{\rm B} = 1550 \text{ nm}$
Grating length	5-8 mm
Grating period	FBG H ₂ sensor, $\Lambda = 520 \text{ nm}$
	FBG CH ₄ sensor, $\Lambda = 550 \text{ nm}$
Fiber core refractive index	$n_{eff} = 1.448$
Wavelength tolerance	±0.5 nm
Reflectance	> 90%
Peak width at -3 dB	$0.25 \sim 0.35 \text{ nm}$
Fiber coating layer	Acrylate
Fiber type	SMF28-compatible
Fiber termination	FC/UPC
Pigtail length	1 m
Grating profile	Anodized
Mechanical test	>100 kpsi
Coated sensing material	Palladium (Pd) and PDMS
	polymer

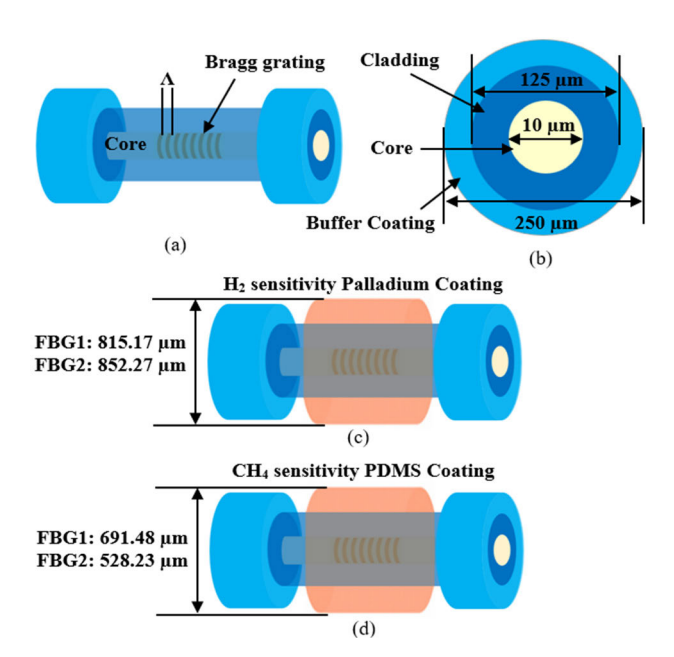


FIGURE 2. Schematic diagram of (a) FBG sensor, (b) cross-sectional area, (c) H_2 FBG sensor coated by Palladium, and (d) CH_4 FBG sensor coated by PDMS polymer.

5 minutes on a microscope glass slide. The exposed core region of the FBG sensor was cleaned with isopropanol, dipped once, and then heat-treated in a CVMS CLIMATIC oven at 60 °C for 6 hours. The coating thicknesses were measured using a Meiji Techno microscope (Model MT4300H). For the palladium-coated FBG sensors, the measured thicknesses were 815.17 μ m and 852.26 μ m for the FBG1H2 and FBG2H2 sensors, respectively. For the PDMS-coated sensors, the thicknesses were 691.48 μ m for FBG1CH4 and 528.23 μ m for FBG2CH4, respectively, as shown in Figs. 4(a)–(d). The coating process was performed manually; therefore, a uniform thickness could not be achieved over the entire 10 mm FBG region. The FBG sensors used in this study were tested for reliability and stability at 90 °C for 1000 hours.



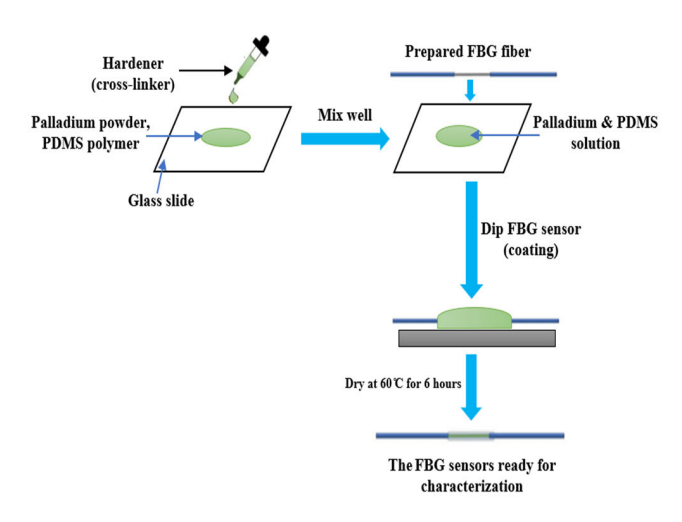


FIGURE 3. The FBG sensors coating process.

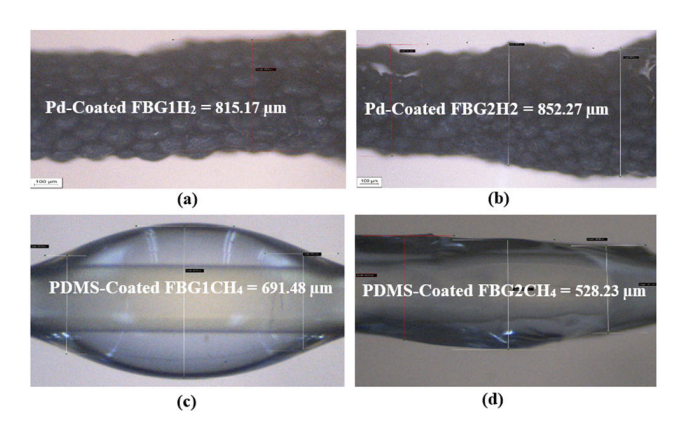


FIGURE 4. Coated FBG sensors observed under the Meiji Techno microscope: (a) Pd-coated FBG1H₂ sensor, (b) Pd-coated FBG2H₂ sensor, (c) PDMS-coated FBG1CH₄ sensor, (d) PDMS-coated FBG2CH₄ sensor.

C. EXPERIMENTAL FRAMEWORK

The experimental setup for measuring hydrogen (H₂) and methane (CH₄) gas concentrations in transformer oil is shown in Fig. 5. The following experimental arrangement was employed at room temperature. A 1000 mL KIMAX KIMBLE test chamber was used and filled with 1020 mL of mineral oil to make sure that there was no room for air during the H₂ and CH₄ injections. The FBG sensors were placed within a smaller, temperature-controlled test chamber. The FBG1H₂ coating was palladium and the FBG2CH₄ coating was PDMS. Then, both sensors were spliced together and connected to an optical spectrum analyzer (Yokokawa, model AQ6370D). An OSA built-in light source at 1550 nm, 22 mW, 50 nm bandwidth, FC/APC connector was utilized to interrogate the proposed FBG sensors. Temperature within the test chambers was monitored using a HERCHR digital thermometer. Measurements were synchronized and recorded using a personal computer (PC). To perform dissolved gas analysis (DGA) of mineral oil, a 50 mL DGA syringe was used to extract oil from a sampling port located near the sensors, allowing analysis with the TRANSPORT X system at the corresponding temperatures.

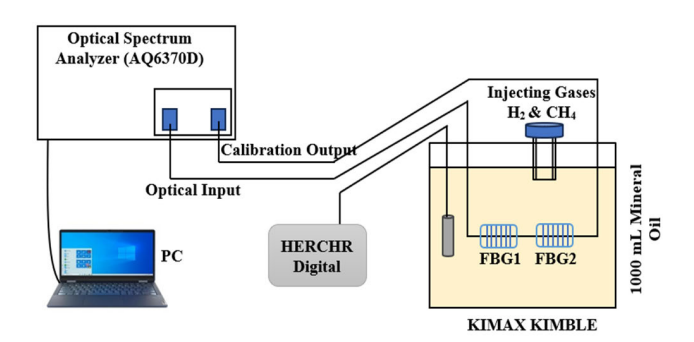


FIGURE 5. FBG sensors schematic circuit diagram of the experimental setup.

D. PREPARATION OF OIL SAMPLES

A one-million part per million (1,000,000 ppm) 99.9% pure hydrogen (H₂) and pure methane (CH₄) gases were obtained from the gas sampling bags, as shown in Fig. 6 (a). The concentration of H₂ and CH₄ in oil was prepared by injecting specific volumes of H2 and CH4 gases from the sampling bags into the 1020 mL mineral oil inside the KIMAX KIM-BLE test chamber using a micro sampler microliter syringe micro-injector equipped with both 100 μ L and 1000 μ L Luer lock removable needles. The KIMAX KIMBLE test bottle was sealed with a GL45 supplementary bottle cap, as shown in Figs. 6 (b) and (c). After each injection of H₂ or CH₄ gas, the bottle was shaken for 10 minutes to ensure the gases were properly dissolved in the oil. A total of 30 oil samples with varying H₂ and CH₄ concentrations were prepared. From each sample, 50 mL of oil was extracted for DGA testing using the TRANSPORT X system, as illustrated in Fig. 7. The FBG sensors response, as the wavelength shift was recorded and matched with the TRANSPORT X results to calibrate the manufactured sensors for detecting the H₂ and CH₄ concentrations in the transformer oil.



FIGURE 6. (a) Gas sampling bags for H₂ and CH₄ gases, (b) Microliter Syringe Micro-injector equipped with both 100 µL and 1000 µL with removable needles, (c) The KIMAX KIMBLE test bottle sealed with a GL45 cap.



FIGURE 7. TRANSPORT X for DGA test.

IV. EXPERIMENTAL RESULTS AND DISCUSSION

A. PALLADIUM-COATED FBG H_2 SENSOR RESPONSE FOR HYDROGEN DETECTION IN MINERAL OIL

The experimental response of the palladium (Pd)-coated FBG1H₂ and FBG2H₂ hydrogen sensors depend on two key factors: hydrogen concentration and temperature in transformer oil. The relationship between the Bragg wavelength shift and hydrogen concentration determines the linearity and sensitivity of the FBG H₂ sensors for detecting dissolved hydrogen gas in mineral oil. The sensors were tested using mineral oil samples with various hydrogen concentrations in the range of 5 ppm to 2146 ppm at room temperature. Each measurement was repeated three times to obtain reliable Bragg wavelength shift values corresponding to each hydrogen concentration. The relationship between the wavelength shift and the H₂ concentration exhibited strong linearity as shown in Fig.8. The response of the two sensors, FBG1H₂ and FBG2H₂, were very close. A clear positive linear correlation is observed between the Bragg wavelength shift (nm) and hydrogen concentration (ppm), as measured by TRANS-PORT X. For the FBG1H₂ sensor, the Pearson correlation coefficient (R) is 0.9878, and the coefficient of determination (R^2) is 0.9757. At the same time, results from FBG2H₂ sensor, yielded Pearson R was 0.9882, and the R^2 was 0.9766. As the FBG1H₂ sensor shows a slightly higher R^2 value, the regression model representing the relationship between the measured Bragg wavelength shift, $\Delta \lambda_B$ and hydrogen concentration obtained from FBG1H2 and FBG2H2 sensors were given by

$$\Delta \lambda_{B_FBG1H_2} = 0.0003 \ C (H_2) - 0.061 \tag{8}$$

$$\Delta \lambda_{B_FBG2H_2} = 0.0003 \ C (H_2) - 0.078 \tag{9}$$

where $\Delta\lambda_{B_FBG1H2}$ and $\Delta\lambda_{B_FBG2H}$ are the Bragg wavelength shift in nm obtained from an FBG1H₂ and an FBG2H₂ sensors, respectively and $C(H_2)$ represents the hydrogen concentration obtained from the TRANSPORT X (ppm). Apart from determining the wavelength shift as a function of H₂ concentration, its relationship as a function of transformer oil temperature was also investigated. The response of the FBG1H₂ and FBG2H₂ sensors was evaluated by injecting 200 mL of hydrogen concentration into the 1020 μ L

of transformer oil. The response was measured across a temperature range of 10 °C to 90 °C as shown in Fig.9. Similarly, the relationship was also strongly linear. The R was 0.9743 for the FBG1H₂ sensor and 0.9753 for the FBG2H₂ sensor, and the R^2 was 0.9492 for FBG1H₂ and 0.9512 for FBG2H₂. This linear relationship indicates that temperature significantly influences the sensors response. Thus, the linear regression representing the relationship between the measured Bragg wavelength shift and oil temperature of FBG1H₂ and FBG2H₂ sensor can be written as:

$$\Delta \lambda_{B_FBG1H_2} = 0.0075 \ T - 0.1543 \tag{10}$$

$$\Delta \lambda_{B_FBG2H_2} = 0.0075 \ T - 0.1555 \tag{11}$$

where $\Delta \lambda_{B_FBG1H2}$ and $\Delta \lambda_{B_FBG2H2}$ are the Bragg wavelength shift in nm obtained from an FBG1H₂ and an FBG2H₂ sensors, respectively, and T is the oil temperature (°C).

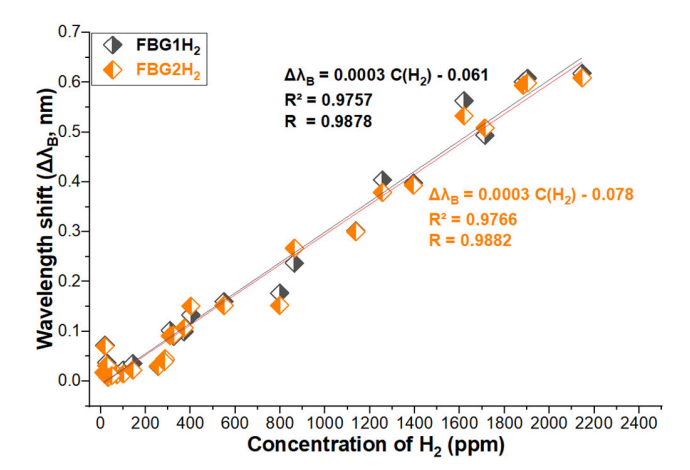


FIGURE 8. The measured Bragg wavelength shift as a function of hydrogen concentration (Pd- coated FBG sensor).

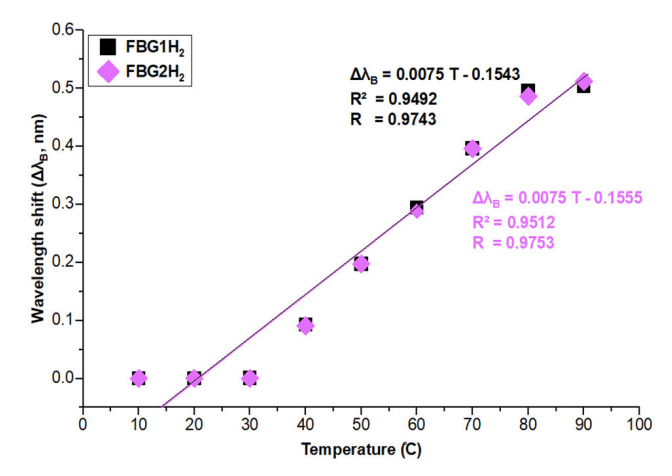


FIGURE 9. The measured Bragg wavelength shift as a function of temperature in the range of 10–90 $^{\circ}$ C after injecting 200 μ L of H₂ concentration into mineral oil.

It is noteworthy that the concentration of H_2 decayed rapidly, as shown in Fig.10. In this figure, the H_2 concentration was injected into the transformer oil. Then the wavelength shift was measured as a function of time. The graphs indicate that the wavelength shift reached its peak



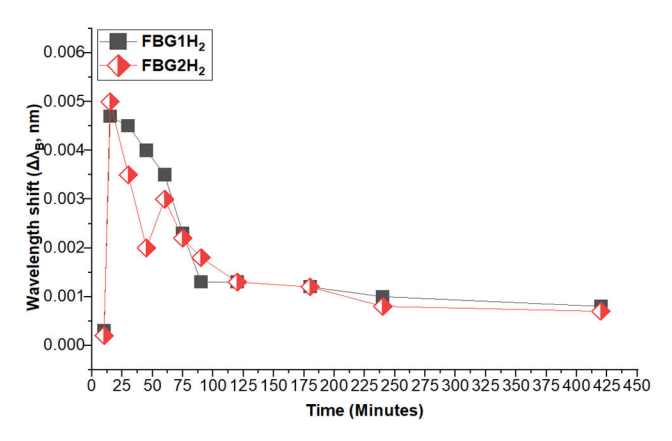


FIGURE 10. Performance of Pd-coated FBG1H $_2$ and FBG2H $_2$ hydrogen sensors in mineral oil after injecting 200 μ L of H $_2$ concentration into mineral oil at room temperature.

approximately 20 minutes after injection. After that, the wavelength shift started to decay. Referred to (7), the concentration of gases will directly depend upon the wavelength shift. This indicates that the concentration of H_2 also peaked at about 20 minutes after injection. Therefore, for testing the H_2 sensor response, the time after injection is very important. The average sensitivities of the FBG1 H_2 and FBG2 H_2 hydrogen sensors could be obtained from the ratio of the measured Bragg wavelength shift ($\Delta \lambda_B$, in nm) to the hydrogen concentration ($C(H_2)$, in ppm), expressed as ($\Delta \lambda_B/C(H_2)$). The calculated sensitivities are 0.000487 nm/ppm for the FBG1 H_2 sensor and 0.000451 nm/ppm for the FBG2 H_2 sensor.

The sensor percentage error was calculated $(\Delta \lambda_{B_absoluteerror} / \Delta \lambda_{B_measured}) \times 100$, where the absolute error in wavelength shift is given by: $\Delta \lambda_{B_absoluteerror} =$ $\Delta \lambda_{B_measured} - \Delta \lambda_{B_predicted}$, and the predicted wavelength shift is derived using Eqs (8) and (9). The difference between the measured value and the calculated value from regression models was 2.964% and 0.047% for the FBG1H₂ and FBG2H₂ sensors, respectively. However, in terms of sensitivity to hydrogen gas, the FBG1H2 sensor demonstrated higher sensitivity than the FBG2H2 sensor, indicating that it undergoes a greater Bragg wavelength shift per unit increase in hydrogen concentration. These results confirm that the sensors, particularly FBG1H₂, are highly suitable for dissolved gas analysis (DGA) in transformer oil, making them effective tools for monitoring hydrogen levels as part of transformer health diagnostics.

B. POLYDIMETHYLSILOXANE POLYMER-COATED FBG SENSORS RESPONSE FOR METHANE DETECTION IN MINERAL OIL

Similar experiments were conducted to examine the response of PDMS coated methane sensors, FBG1CH₄ and FBG2CH₄, in detecting CH₄ concentration in transformer oil. The wavelength shifts of both sensors as function of CH₄ concentration and temperature are shown in Figs. 11-13 respectively. In Fig.11, the wavelength shifts as a function of CH₄ concentration in the ranging from 3 ppm up to 1551 ppm, is also

linear, similar to the case of H_2 sensors. For the FBG1CH₄ sensor, the R is 0.9715, and R^2 is 0.9438. For the FBG2CH₄ sensor, the R is 0.9881, and the R^2 is 0.9763. The regression models describing the relationship between the measured Bragg wavelength shift and CH₄ concentration, as obtained from the FBG1CH₄ and FBG2CH₄ sensors, are presented as

$$\Delta \lambda_{B_FBG1CH_4} = 0.0005 \ C \ (CH_4) + 0.2089$$
 (12)

$$\Delta \lambda_{B \ FBG2CH_4} = 0.0005 \ C \ (CH_4) + 0.0442$$
 (13)

where $\Delta \lambda_{B_FBG1CH4}$ and $\Delta \lambda_{B_FBG2CH4}$ denote the Bragg wavelength shift in unit of nm of FBG1CH₄ and FBG2CH₄ sensors, respectively, while $C(CH_4)$ is the methane concentration obtained from the TRANSPORT x in ppm.

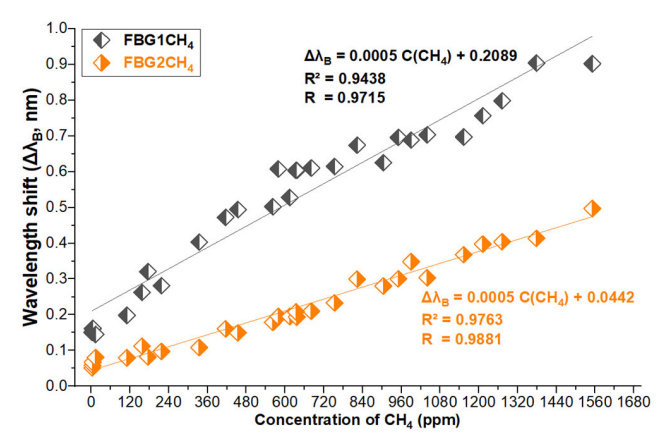


FIGURE 11. The measured Bragg wavelength shift as a function of methane concentration (PDMS-coated FBG).

In addition to examining how the wavelength shift varies with CH₄ concentration, we also explored its relationship with the temperature of transformer oil. The responses of the FBG1CH₄ and FBG2CH₄ sensors were evaluated by injecting 200 μ L of methane into 1020 mL of transformer oil. Measurements were taken across a temperature range of 10 °C to 90 °C, as illustrated in Fig. 12. The observed relationship was notably strong and linear. The R was 0.9854 for the FBG1CH₄ sensor and 0.9847 for the FBG2CH₄ sensor. The R^2 were 0.9710 for a FBG1CH₄ sensor and 0.9763 for a FBG2CH₄ sensor. The linear regression analysis confirms a significant influence of oil temperature on the sensor response. The regression models describing the relationship between the measured Bragg wavelength shift and oil temperature for the FBG1CH4 and FBG2CH4 sensors are presented by

$$\Delta \lambda_{B_FBG1CH_4} = 0.0088 \ T - 0.1514 \tag{14}$$

$$\Delta \lambda_{B \ FBG2CH_A} = 0.0095 \ T - 0.2641 \tag{15}$$

where $\Delta \lambda_{B_FBG1CH4}$ is the measured Bragg wavelength shift in nm of a FBG1CH₄ sensor, $\Delta \lambda_{B_FBG2CH4}$ is the Bragg wavelength shift in nm of a FBG2CH₄ sensor, and T is the oil temperature in Celsius.

The wavelength shifts for the two sensors as a function of time after injecting CH_4 into the transformer oil are displayed in Fig. 13. The response is very similar to that of the H_2 case,

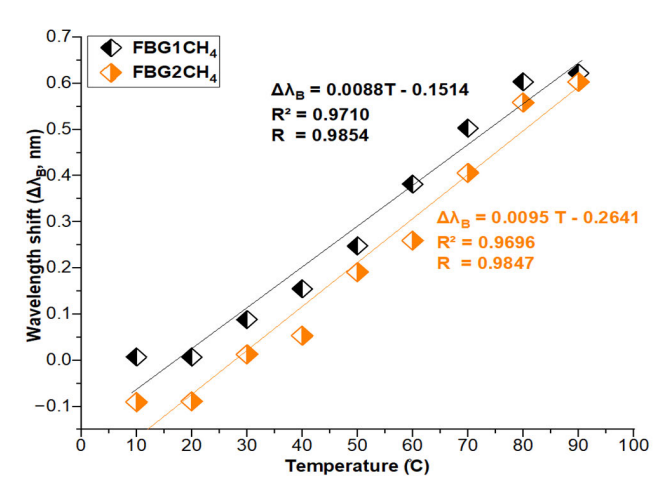


FIGURE 12. Measured Bragg wavelength shifts as a function of temperature in the range of 10–90 °C after injecting 200 μ L of CH₄ into mineral oil.

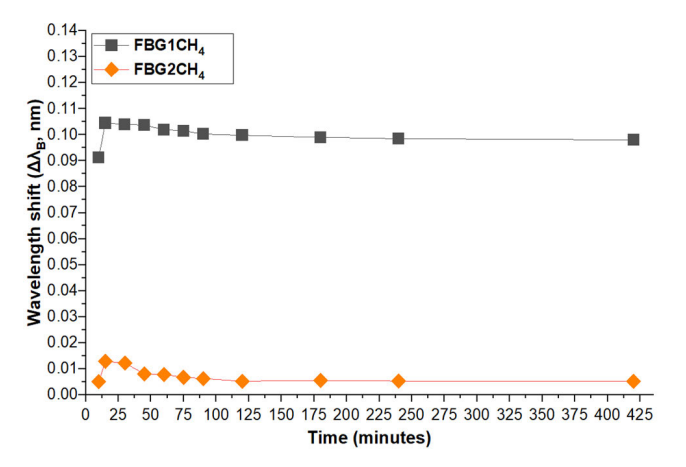


FIGURE 13. Performance of PDMS-coated FBG1CH₄ and FBG2CH₄ methane sensors in mineral oil after injecting of 200 μ L of CH₄ concentration into mineral oil at room temperature.

with the peak reached approximately 20 minutes after injection. Then, after about 100 minutes, the concentration of CH₄ appears to be constant. Thus, the results of Figs. 11 and 12 were obtained 20 minutes after injecting CH₄ into oil. However, it is noteworthy to observe that the responses of the two sensors differ significantly from each other. Then, the average sensitivity of the FBG1CH4 and FBG2CH4 methane sensors was also determined using the same principle as the case of H₂. The sensitivity of an FBG1CH₄ sensor was 0.005906 nm/ppm, which exceeded that of an FBG2CH₄ sensor, which was 0.002260 nm/ppm. To analyze the difference between the two sensors, the coated film thicknesses of both sensors were measured, as shown in Fig. 4, which revealed that the thicknesses of the PDMS coatings were significantly different: 691.483 μ m and 528.230 μ m for the FBG1CH₄ and FBG2CH4 sensors, respectively. The thickness difference surely affects the sensor's response. The film thickness had been controlled as well as possible, but, unfortunately, maintaining uniform thickness across both sensors proved difficult. A thicker PDMS layer enhances gas absorption

capacity by providing a larger interaction volume for CH₄ molecules. As methane diffuses into the polymer, it induces more significant swelling, which in turn transfers greater strain to the FBG, resulting in a more pronounced Bragg wavelength shifts the difference between the measured values and the calculated values in Eqs. (12) and (13) are 4.151% for the FBG1CH₄ sensor and 4.975% for the FBG2CH₄ sensor. Therefore, the enhanced response of FBG1CH₄ is consistent with the principle that increased coating thickness improves sensor sensitivity.

C. FBG H₂ AND CH₄ SENSOR REPEATABILITY

To measure the repeatability of the sensors, approximately 200 μ L of H₂ and CH₄ were injected into the test chamber, and the values of $\Delta\lambda_B$ were investigated at temperatures of 30 °C, 40 °C, 60 °C, and 90 °C. The experiment was conducted continuously for 10 hours at each temperature for each gas. Repeatability performance was assessed by examining the consistency of the Bragg wavelength shifts. The results revealed minimal variation in the measured shifts, indicating high repeatability, as shown in Fig. 14. The relative standard deviation (*RSD*) was calculated using Eq.(16) [30], [31], where *RSD* is defined as the ratio of the standard deviation (*SD*) of the recorded wavelength shifts to the mean value (C_m), multiplied by 100 to express it as a percentage.

$$\%RSD = \frac{SD}{C_m} \times 100\% \tag{16}$$

A total of 40 samples were collected for each sensor for both hydrogen and methane detections. According to [32], repeatability is considered acceptable when the *RSD* is less than 2%. The calculated *RSD* values at different temperatures are summarized in Table 2. At 40 °C, 60 °C, and 90 °C, the *RSD* values for all sensors were well below 1%, indicating excellent repeatability. At 30 °C, the *RSD* values for the FBG1H₂ and FBG2H₂ sensors were relatively higher due to the small mean wavelength shifts (0.0009 nm and 0.00087 nm, respectively), as this temperature is close to room temperature, resulting in a higher relative variation.

TABLE 2. Repeatability of Fiber Bragg Grating (FBG) Sensors at 30 °C, 40 °C, 60 °C, and 90 °C with 200 μ L H₂ and CH₄ injection.

Temperature	RSD (%)					
(C)	FBG1H ₂	FBG2H ₂	FBG1CH ₄	FBG2CH ₄		
30	5.5479	5.5523	0.0680	0.4102		
40	0.2331	0.3824	0.1997	0.4208		
60	0.3453	0.3294	0.2558	0.1108		
90	0.5799	0.5078	0.6893	0.3414		

TABLE 3. Fiber Bragg Grating (FBG) sensors senstivity at temperature.

Temperature	Sensitivity (nm/℃)					
(C)	FBG1H ₂	FBG2H ₂	FBG1CH ₄	FBG2CH ₄		
30	0.000032	0.000029	0.003267	0.000428		
40	0.002319	0.002269	0.003993	0.001595		
60	0.004939	0.004939	0.006722	0.005126		
90	0.005621	0.005555	0.006913	0.006713		



References	Structure	Detection range (ppm)		Accuracy (%)		Sensitivity (pm/ppm)	
		H_2	$\mathrm{CH_{4}}$	H_2	$\mathrm{CH_4}$	H_2	$\mathrm{CH_4}$
This work	FBG coated by Pd and PDMS sensors	5-2146	3-1551	97.04	95.85	0.4870	5.9070
[15]	FBG-based hydrogen sensor with side- polished and sputtered with palladium/silver.	0 -700	N/A	86.60	N/A	0.4770	N/A
[19]	Palladium-based fiber-optic hydrogen sensor	100-50,000	N/A	96.00	N/A	0.2889	N/A
[20]	Pd/Ag-coated long-period fiber gratings (LPFGs) hydrogen sensor	4,000-11,000	N/A	95.77	N/A	0.3030	N/A
[21]	The fiber Bragg gratings sensors based on different palladium- coatings ratios,	0-700	N/A	81.00	N/A	0.0369	N/A
[29]	Fiber Bragg grating hydrogen sensor based on the Pd/Ni composite film	0-10000	N/A	93.60	N/A	0.0125	N/A

TABLE 4. Comparative study of the proposed Fiber Bragg Grating (FBG) sensors with other similar reported sensors.

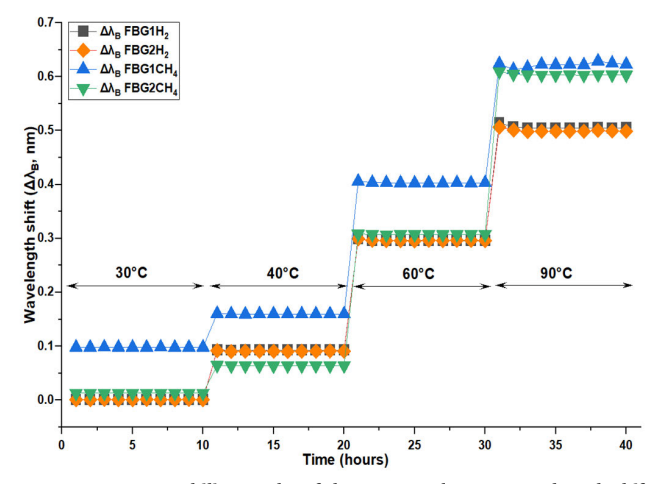


FIGURE 14. Repeatability results of the measured Bragg wavelength shift for FBG1H₂, FBG2H₂, FBG1CH₄, and FBG2CH₄ sensors at 30 °C, 40 °C 60 °C, and 90 °C.

The use of FBG1H₂ and FBG2H₂ sensors at 30 °C can be considered carefully and may be unnecessary, given that the normal transformer's operating temperature is significantly higher. These findings confirm that the Pd- and PDMS-coated FBG sensors exhibit strong repeatability under controlled conditions, reinforcing their reliability for continuous, real-time monitoring of dissolved hydrogen and methane gases in transformer oil.

D. SENSITIVITY CALIBRATION AT DIFFERENT TEMPERATURES

To measure the sensitivity of the sensors, approximately 200 ppm gas concentrations of $\rm H_2$ and $\rm CH_4$ were injected into the test chamber separately for each sensor. The oven temperature was set at 30 °C, and the Bragg wavelength shifts were later observed and recorded. The sensor sensitivity is defined as the ratio of the Bragg wavelength shift to the test temperature, expressed in nm/°C. The furnace temperature was adjusted progressively, starting at 30 °C and subsequently increasing to 40 °C, 60 °C, and finally 90 °C. The corresponding sensitivity values across this temperature range are presented in Fig. 15. The sensor sensitivity in this figure is best described by a logarithmic relationship with the temperature. The R^2 of FBG1H₂ and FBG2H₂ are 0.930 and

0.927, respectively, while those of FBG1CH₄ and FBG2CH₄ sensors are 0.974 and 0.897, respectively. These sensitivities were obtained from the same data measured in Section C. The sensitivity of each sensor clearly depends upon the temperature, as the higher the temperature, the greater the sensitivity. For $\rm H_2$ sensors, the sensitivities of both sensors are very close. In contrast, the sensitivity of the CH₄ sensor indicates that the FBG1CH₄ sensor exhibits a noticeably higher sensitivity value at 30 °C, and this difference decreases as the temperature increases. It is noteworthy that the sensitivity of both CH₄ sensors is very close at 90 °C.

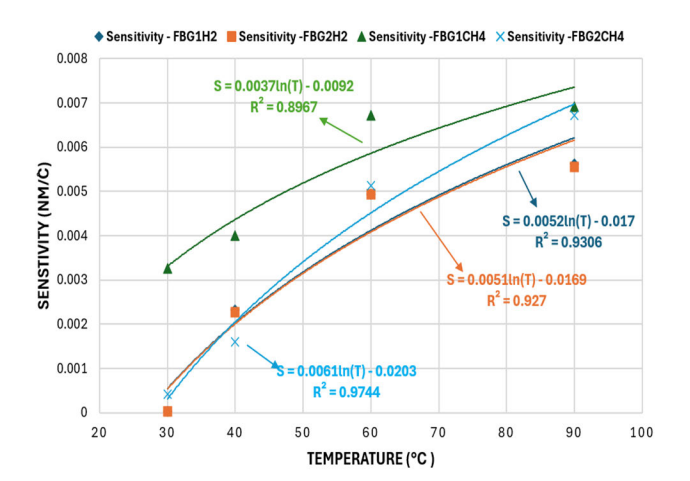


FIGURE 15. FBG H₂ and CH₄ sensors sensitivity as a function of temperature.

E. FBG H₂ AND CH₄ SENSORS PERFORMANCE

The developed FBG sensors achieved sensitivities for H₂ and CH₄ concentrations as given in Section IV. The sensor sensitivities at different temperatures, presented in Table 3, surpass those of many previously reported FBG-based and Pd-coated sensors in terms of sensitivity, detection range, and accuracy. Table 4 presents a comparative analysis of various FBG-based sensors used for 2 and CH₄ detection in transformer oil. In contrast, other sensor types including side-polished FBG-based hydrogen sensors [15], palladium-based fiber-optic hydrogen sensors, and long-period gratings (LPGs) coated with Pd/Ag layers [19], [20], as well as FBG sensors using different palladium (Pd) coating ratios



and Pd/Ni composite films [21], [29] generally demonstrate lower sensitivities, narrower detection ranges, and moderate accuracy. The proposed Pd- and PDMS-coated FBG sensors demonstrate advantages in sensitivity, repeatability, and environmental stability, making them strong candidates for continuous, accurate monitoring of hydrogen and methane concentrations in transformer oil, thereby contributing to improved transformer health diagnostics.

V. CONCLUSION

In this study, Fiber Bragg Grating (FBG) sensors coated with palladium (Pd) and polydimethylsiloxane (PDMS) were successfully developed and evaluated for the detection of dissolved hydrogen (H₂) and methane (CH₄) in transformer oil. The sensors exhibited excellent linear sensitivity across wide concentration ranges, 5-2146 ppm for H₂ and 3-1551 ppm for CH₄ and maintained consistent performance under varying temperature conditions. Temperature correction models were established to ensure accurate gas detection under practical transformer operating environments. The sensors demonstrated high sensitivity and strong linearity, with sensitivities of 0.000487 nm/ppm and 0.000451 nm/ppm for the FBG1H₂ and FBG2H₂ sensors, respectively, and 0.005906 nm/ppm and 0.002260 nm/ppm for the FBG1CH₄ and FBG2CH₄ sensors, respectively. Repeatability tests showed excellent consistency. The Pd coated sensors showed superior performance in H₂ detection, while the PDMS-coated sensors were effective for CH₄ monitoring. Compared to other optical fiber-based gas sensors, the proposed FBG sensors demonstrated enhanced sensitivity, broader detection range, and improved response stability. These findings confirm the suitability of the developed sensors for real-time, long-term monitoring of dissolved gases in transformers, contributing to enhanced fault diagnostics and operational safety. Future work will focus on integrating the developed sensors into commercial transformer systems for field validation and long-term durability assessment. Key challenges include improving coating uniformity, enhancing sensor selectivity in multi-gas environments, and developing multiplexed FBG arrays for simultaneous detection of multiple dissolved gases.

ACKNOWLEDGMENT

The authors would like to express their sincere gratitude to the Petchra Pra Jom Klao Ph.D. Research Scholarship from the King Mongkut's University of Technology Thonburi (KMUTT) for the support of this research. They would also like to thank Charoenchai Transformer Company Ltd., for providing access to the Transformer X machine for sampling and Dissolved Gas Analysis (DGA) testing, as well as for supplying transformer oil.

REFERENCES

[1] C. Gao, B. Qi, Y. Gao, Z. Zhu, and C. Li, "Kerr electro-optic sensor for electric field in large-scale oil-pressboard insulation structure," *IEEE Trans. Instrum. Meas.*, vol. 68, no. 10, pp. 3626–3634, Oct. 2019, doi: 10.1109/TIM.2018.2881803.

- [2] M. Duval, "Dissolved gas analysis: It can save your transformer," IEEE Elect. Insul. Mag., vol. 5, no. 6, pp. 22–27, Nov. 1989, doi: 10.1109/57.44605.
- [3] K. Wang, X. Tong, and X. Zhu, "Transformer partial discharge monitoring based on optical fiber sensing," *Photonic Sensors*, vol. 4, no. 2, pp. 137–141, Jun. 2014, doi: 10.1007/s13320-014-0181-4.
- [4] Q. Su, C. Mi, L. L. Lai, and P. Austin, "A fuzzy dissolved gas analysis method for the diagnosis of multiple incipient faults in a transformer," *IEEE Trans. Power Syst.*, vol. 15, no. 2, pp. 593–598, May 2000, doi: 10.1109/59.867146.
- [5] Y. R. S. J. Singh and P. Verma, "Dissolved gas analysis for transformers," *Electr. India*, vol. 47, no. 10, p. 72, 2007.
- [6] K. Chen, M. Guo, B. Yang, F. Jin, G. Wang, F. Ma, C. Li, B. Zhang, H. Deng, and Z. Gong, "Highly sensitive optical fiber photoacoustic sensor for in situ detection of dissolved gas in oil," *IEEE Trans. Instrum. Meas.*, vol. 70, pp. 1–8, 2021, doi: 10.1109/TIM.2021.3102746.
- [7] F. Rastrello, P. Placidi, A. Scorzoni, E. Cozzani, M. Messina, I. Elmi, S. Zampolli, and G. C. Cardinali, "Thermal conductivity detector for gas chromatography: Very wide gain range acquisition system and experimental measurements," *IEEE Trans. Instrum. Meas.*, vol. 62, no. 5, pp. 974–981, May 2013, doi: 10.1109/TIM.2012.2236723.
- [8] Z. Yuan, H. Zhang, J. Li, F. Meng, Z. Yang, and H. Zhang, "Ag nanoparticle-modified ZnO-In₂O₃ nanocomposites for low-temperature rapid detection hydrogen gas sensors," *IEEE Trans. Instrum. Meas.*, vol. 72, pp. 1–12, 2023, doi: 10.1109/TIM.2023.3243681.
- [9] S.-Y. Chiu, H.-W. Huang, T.-H. Huang, K.-C. Liang, K.-P. Liu, J.-H. Tsai, and W.-S. Lour, "High-sensitivity metal–semiconductor–metal hydrogen sensors with a mixture of Pd and SiO₂ forming three-dimensional dipoles," *IEEE Electron Device Lett.*, vol. 29, no. 12, pp. 1328–1331, Dec. 2008, doi: 10.1109/LED.2008.2006994.
- [10] Z. Chen, X. Zhang, H. Cheng, Y. Zhang, T. Yang, and Y. Zhang, "Study on photoacoustic spectroscopy detection of CO in gas insulation equipment," *IEEE Trans. Dielectr. Electr. Insul.*, vol. 29, no. 4, pp. 1498–1505, Aug. 2022, doi: 10.1109/TDEI.2022.3178059.
- [11] X. Zhao, K. Chen, M. Guo, C. Li, C. Li, G. Zhang, Z. Gong, Z. Zhou, and W. Peng, "Ultra-high sensitive multipass absorption enhanced fiber-optic photoacoustic gas analyzer," *IEEE Trans. Instrum. Meas.*, vol. 72, pp. 1–8, 2023, doi: 10.1109/TIM.2022.3188043.
- [12] J. Gao, Y. Zhang, X. Li, G. Shi, and Y. Zhang, "Quantitative detection of multicomponent SF₆ decomposition products based on Fourier transform infrared spectroscopy combined with CARS-ELM algorithm," *IEEE Trans. Instrum. Meas.*, vol. 71, pp. 1–8, 2022, doi: 10.1109/TIM.2022.3194933.
- [13] W. Chen, Z. Gu, J. Zou, F. Wan, and Y. Xiang, "Analysis of furfural dissolved in transformer oil based on confocal laser Raman spectroscopy," *IEEE Trans. Dielectr. Electr. Insul.*, vol. 23, no. 2, pp. 915–921, Apr. 2016, doi: 10.1109/TDEI.2015.005434.
- [14] K. Schroeder, W. Ecke, and R. Willsch, "Optical fiber Bragg grating hydrogen sensor based on evanescent-field interaction with palladium thin-film transducer," *Opt. Lasers Eng.*, vol. 47, no. 10, pp. 1018–1022, Oct. 2009, doi: 10.1016/j.optlaseng.2009.04.002.
- [15] J. Jiang, G.-M. Ma, C.-R. Li, H.-T. Song, Y.-T. Luo, and H.-B. Wang, "Highly sensitive dissolved hydrogen sensor based on side-polished fiber Bragg grating," *IEEE Photon. Technol. Lett.*, vol. 27, no. 13, pp. 1453–1456, Jul. 15, 2015, doi: 10.1109/LPT.2015.2425894.
- [16] A. Trouillet, E. Marin, and C. Veillas, "Fibre gratings for hydrogen sensing," *Meas. Sci. Technol.*, vol. 17, no. 5, pp. 1124–1128, May 2006, doi: 10.1088/0957-0233/17/5/s31.
- [17] D. Y. Wang, Y. Wang, J. Gong, and A. Wang, "Fully distributed fiber-optic hydrogen sensing using acoustically induced long-period grating," *IEEE Photon. Technol. Lett.*, vol. 23, no. 11, pp. 733–735, Jun. 1, 2011, doi: 10.1109/LPT.2011.2131644.
- [18] N. Basumallick, P. Biswas, R. M. Carter, R. R. J. Maier, S. Bandyopadhyay, K. Dasgupta, and S. Bandyopadhyay, "Design of palladium-coated longperiod fiber grating for hydrogen sensing," *J. Lightw. Technol.*, vol. 34, no. 21, pp. 4912–4919, Nov. 15, 2016, doi: 10.1109/JLT.2016.2604481.
- [19] M. Fisser, R. A. Badcock, P. D. Teal, and A. Hunze, "High-sensitivity fiber-optic sensor for hydrogen detection in gas and transformer oil," *IEEE Sensors J.*, vol. 19, no. 9, pp. 3348–3357, May 2019, doi: 10.1109/JSEN.2019.2891523.
- [20] K. Zhu, B. Qi, M. Ji, M. Huang, C. Gao, X. Yang, H. Jin, and C. Li, "A highly sensitive and durable sensor for in situ hydrogen measurement in transformer oil," *IEEE Trans. Instrum. Meas.*, vol. 73, pp. 1–8, 2024, doi: 10.1109/TIM.2024.3470057.



- [21] M. R. Samsudin, Y. G. Shee, F. R. M. Adikan, B. B. A. Razak, and M. Dahari, "Fiber Bragg gratings hydrogen sensor for monitoring the degradation of transformer oil," *IEEE Sensors J.*, vol. 16, no. 9, pp. 2993–2999, May 2016, doi: 10.1109/JSEN.2016.2517214.
- [22] X. Ping, X. Cao, C. Cao, H. Lei, C. Yang, Q. Cheng, T. Zhou, and M. Liu, "Fiber grating hydrogen sensor: Progress, challenge and prospect," Adv. Sensor Res., vol. 3, no. 2, Feb. 2024, Art. no. 2300088, doi: 10.1002/adsr.202300088.
- [23] M. Bhattarai, "Active hydrogen sensing using a palladium coated optical fiber Bragg grating sensor," Ph.D. dissertation, Dept. Elect. Eng., Univ. Pittsburgh, Pittsburgh, PA, USA, 2007.
- [24] M. M. Wemeck, R. Allil, B. A. Ribeiro, and F. V. De Nazare, "A guide to fiber Bragg grating sensors," in *Current Trends in Short—and Long-Period Fiber Gratings*, C. A. C.-Laborde, Ed., London, U.K.: IntechOpen, May 2013, doi: 10.5772/54682.
- [25] J. C. C. Da Silva and H. J. Kalinowski, "Strain studies in electrical energy transmission cables using an optical fiber Bragg grating sensor," in *IEEE MTT-S Int. Microw. Symp. Dig.*, vol. 1, Aug. 2001, pp. 313–316, doi: 10.1109/SBMOMO.2001.1008773.
- [26] A. J. Swanson, "Sensors for optics-based strain, temperature and chemical sensing," M.S. thesis, Dept. Physics, Massey Univ., Palmerston North, New Zealand, 2015. [Online]. Available: https://mro.massey.ac.nz/bitstreams/download
- [27] S. L. S. A. J. McCarty. (2025). Biophysical Chemistry. Bellingham. [Online]. Available: https://chem.libretexts.org/@go/page/398298
- [28] M. Chauhan, T. Khanikar, and V. K. Singh, "PDMS coated fiber optic sensor for efficient detection of fuel adulteration," *Appl. Phys. B*, vol. 128, no. 4, p. 89, Apr. 2022, doi: 10.1007/s00340-022-07809-8.
- [29] F. Xiang, G. Wang, Y. Qin, S. Yang, X. Zhong, J. Dai, and M. Yang, "Improved performance of fiber Bragg hydrogen sensors assisted by controllable optical heating system," *IEEE Photon. Technol. Lett.*, vol. 29, no. 15, pp. 1233–1236, Aug. 15, 2017, doi: 10.1109/LPT.2017.2701840.
- [30] S. Belouafa, F. Habti, S. Benhar, B. Belafkih, S. Tayane, S. Hamdouch, A. Bennamara, and A. Abourriche, "Statistical tools and approaches to validate analytical methods: Methodology and practical examples," *Int. J. Metrology Quality Eng.*, vol. 8, p. 9, Jan. 2017, doi: 10.1051/ijmqe/2016030.
- [31] D. C. Montgomery and G. C. Runger, "Applied statistics and probability for engineers," in *Applied Statistics and Probability for Engineers*, 3rd ed., Hoboken, NJ, USA: Wiley, 2003.
- [32] J. M. Green, "A practical guide to analytical method validation," Anal. Chem. News Features, vol. 68, no. 9, pp. 305–309, May 1, 1996.



FOLAD FAWAD (Graduate Student Member, IEEE) received the B.Eng. degree in electrical and electronics engineering from Jawaharlal Nehru Technological University, Hyderabad, India, in 2017, and the M.Eng. degree in electrical and information engineering from the King Mongkut's University of Technology Thonburi, Bangkok Thailand, in 2021, where he is currently pursuing the Ph.D. degree in electrical and information engineering technology. His main

research interests include high-voltage, transformer insulation testing, and transformer testing in electrical engineering field.



SUPAKIT CHOTIGO received the B.Eng. degree in electrical engineering from KMUTT and the master's and Ph.D. degrees from the University of Manchester Institute of Science and Technology (UMIST), U.K. He is currently a Faculty Member with the Department of Electrical Engineering, KMUTT, and formerly, he was the Department Head, from 2011 to 2019. He has extensive experience in teaching, research, and national-level engineering consultancy, especially in high-voltage

systems, underground cable transition projects, transformer testing, and the development of sustainable natural ester transformer oil. Over the past five years, his recent research interests include moisture detection in transformer oil, electrical cable condition assessment, energy conservation techniques, and electrical safety technology, with publications in both domestic and international conferences and journals.



APICHAI BHATRANAND received the B.Eng. degree in electrical engineering from Mahidol University, Thailand, and the M.Eng. and Ph.D. degrees in electrical engineering from Texas A&M University, College Station, TX, USA.

From 1999 to 2004, he was a Research Assistant with the Electrical Engineering Department, Texas A&M University. Since 2004, he has been a Lecturer with the Electronic and Telecommunication Engineering Department, King Mongkut's Univer-

sity of Technology Thonburi, Thailand. His research interests include optical sensors, optical communications, integrated optics, biomedical sensors, and other related topics in optics and bioengineering.



SARAYUT YONGPRAPAT received the B.Sc. degree in chemistry from Thammasat University, Thailand, and the M.Sc. and Ph.D. degrees in energy technology from The Joint Graduate School of Energy and Environment (JGSEE), King Mongkut's University of Technology Thonburi (KMUTT), Thailand.

During the period from 2014 to 2019, and since 2022, he has been a Researcher with the Pilot Plant Development and Training Institute (PDTI),

KMUTT. His research interests include catalysis, electrochemical devices, and their various applications, including fuel cells, CO2RR, electrodeposition, and other topics related to analytical chemistry.



SANGUAN ANANTATHANASARN received the Ph.D. degree from the Graduate School of Electronics and Information Engineering, Hokkaido University, Japan, in 2003. From 2004 to 2008, he was with Eindhoven University of Technology, The Netherlands, where he developed continuous-wave quantum dot lasers for 1.55 μ m telecommunication. He is currently the Research and Development Center General Manager and the Chief Technology Officer with Furukawa FITEL

(Thailand) Company, Ltd. His research interests include electronic and photonic devices, optoelectronic packaging technologies, and artificial intelligence.



RATTANAPORN SUKSOMBOON received the B.Eng. degree in electronics and telecommunication engineering from the King Mongkut's University of Technology Thonburi, Thailand, in 2004, and the M.Eng. degree in industrial management engineering from Thammasat University, Thailand, in 2011. She is currently with the Research and Development Center, Furukawa FITEL (Thailand) Company Ltd. Her research interests include fiber Bragg grating, laser diode

packaging, and digital twin for next-generation manufacturing.

VOLUME 13, 2025 182855

. . .